Synthesis, Structure and Properties of Lanthanide-Organic Frameworks with Imidazolylmethylisophthalate Ligands

Xiao-Chun Cheng and Xiao-Hong Zhu

Faculty of Life Science and Chemical Engineering, Huaiyin Institute of Technology, Huaian 223003, P. R. China

Reprint requests to Dr. Xiao-Hong Zhu. Fax: +86-517-83559044. E-mail: hgzhuxh@yeah.net

Z. Naturforsch. **2013**, *68b*, 1233 – 1238 / DOI: 10.5560/ZNB.2013-3186
Received June 18, 2013

Three new lanthanide-organic frameworks $\{[Ln(L)(OClO_3)(H_2O)]\cdot 0.5H_2O\}_n$ [Ln = Sm (**1**), Eu (**2**), Er (**3**)] have been prepared by hydrothermal reactions of the corresponding lanthanide oxide (Ln_2O_3), silver perchlorate ($AgClO_4$) and 5-(imidazol-1-ylmethyl)isophthalic acid. The complexes have been characterized by single-crystal and powder X-ray diffraction, IR spectroscopy, and elemental analyses. In **1**–**3**, the metal centers are eight-coordinated to show polyhedral coordination geometries with an LnO_8 donor set. The imidazolyl groups are free of coordination, and the perchlorate and carboxylate groups bridge the Ln^{3+} cations leading to the formation of wave-like layer structures containing metal-chains. The fluorescence properties of complex **2** were investigated.

Key words: Lanthanide(III), Isophthalate, Imidazolyl Ligand, Fluorescence

Introduction

In the past decades, supramolecular coordination chemistry has been increasingly focused on, which is justified due to the fascinating architectures and many potential applications [1 – 3]. Consequently, a great number of metal-organic frameworks (MOFs) with various structural features and interesting functional properties have been prepared and discussed in some comprehensive reviews [4 – 6]. Recently, lanthanide-organic supramolecular architectures have attracted increasing attention because of their unusual optical and electronic properties [7 – 9]. Compared with the fruitful production of transition metal-containing coordination polymers, the design and assembly of lanthanide-organic frameworks (LOFs) has remained less developed.

Coordination polymers based on carboxylate-containing ligands have been extensively studied, since carboxylate groups can exhibit variable coordination modes which can enrich the variation of the resulting structures beneficial to the achievement of diverse properties of a vast domain of potentially multifunctional materials [10 – 12]. It is known that lanthanide ions generally show higher affinity to oxygen atoms than to nitrogen atoms. Therefore, for the formation of LOFs *O*-donor ligands seem to be preferable over other types such as mixed *N*- and *O*-donor ligand. Although *N*-donor coordination groups are poor donors to lanthanides, they are more inclined to transition metals such as silver to form a linear N–Ag–N coordination geometry. Thus, synthetic strategies can be attempted to pursue new heterometallic coordination in crystal engineering. In this paper, V-shaped imidazolyl-containing isophthalic acid (H_2L) was used to bridge the lanthanide ions and to form inorganic-organic hybrid frameworks. As a mixed *N*- and *O*-donor ligand, H_2L can be used for heterometallic systems, namely transition and lanthanide metals. Given the subtlety of the assembly process, the resulting complexes may be expected to contain only transition or only lanthanide metals, or both of them. Flexible imidazolylmethyl groups can enrich the coordination variety due to their free axial rotation [13 – 15]. Three new lanthanide coordination polymers $\{[Ln(L)(OClO_3)(H_2O)]\cdot 0.5H_2O\}_n$ [Ln = Sm (**1**), Eu (**2**), Er (**3**)] have been obtained. The fluorescence properties of complex **2** were investigated in solid state at room temperature.

Results and Discussion

Preparation

Complexes **1**–**3** were readily prepared by hydrothermal reactions of the corresponding lanthanide oxide (Ln_2O_3) with silver perchlorate ($AgClO_4$) and the H_2L ligand at 140 °C. It is noteworthy that Ag(I) ions were not found in the resulting complexes. However, they seem to play an important role in the formation of complexes **1**–**3**, since no crystalline materials were observed if other perchlorate salts were used, such as $Cu(ClO_4)_2$, $Zn(ClO_4)_2$ or $Cd(ClO_4)_2$. Using lanthanide nitrates as starting materials was also not successful.

*Structural description of {[Ln(L)(OClO$_3$)(H$_2$O)]·0.5H$_2$O}$_n$ [Ln = Sm (**1**), Eu (**2**), Er (**3**)]*

Determination of the structures of complexes **1**–**3** by X-ray crystallography has shown that complexes **1**–**3** are isostructural. All three complexes crystallize in the monoclinic system with space group $P2_1/c$ with $Z = 4$ (Table 1). Thus, only the structure of complex **3** will be discussed in detail here.

The H_2L ligand was deprotonated to generate a L^{2-} anion. There are one Er(III), one L^{2-}, one coordinated perchlorate anion, one coordinated water molecule and one half of a non-coordinated water molecule in the asymmetric unit of **3**. As shown in Fig. 1a, each Er(III) is eight-coordinated by four $O_{carboxylate}$ atoms from four different L^{2-} ligands, three $O_{perchlorate}$ atoms from two different perchlorate anions, and one O atom of a coordinated water molecule to furnish a distorted square-antiprismatic coordination geometry with an [ErO_8] donor set (Fig. 1b). The bond lengths and angles around each Er(III) atom are in the range of 2.234(2) – 2.539(2) Å and 57.16(7)–152.86(8)° , respectively (Table 2), which are comparable to those in reported Er(III)-carboxylate complexes. Both carboxylate groups of each L^{2-} ligand exhibit a μ_2-η^1 : η^1-bridging coordination mode (Scheme 1), while each imidazolylmethyl group is free of coordination to lanthanide ions. Thus, in complex **3** each L^{2-} ligand acts as a μ_4-bridge adopting the η^1 : η^1-η^1 : η^1 coordina-

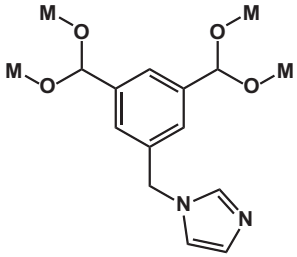

Scheme 1. The coordination mode of the L^{2-} ligand appearing in complexes **1**–**3**.

Table 1. Crystal structure data for **1**–**3**.

	1	**2**	**3**
Empirical formula	$C_{12}H_{11}ClN_2O_{9.5}Sm$	$C_{12}H_{11}ClN_2O_{9.5}Eu$	$C_{12}H_{11}ClN_2O_{9.5}Er$
M_r	521.03	522.64	537.94
Crystal size, mm^3	0.25 × 0.20 × 0.02	0.15 × 0.15 × 0.02	0.20 × 0.20 × 0.05
Crystal system	monoclinic	monoclinic	monoclinic
Space group	$P2_1/c$	$P2_1/c$	$P2_1/c$
a, Å	13.238(5)	13.209(4)	13.180(4)
b, Å	13.067(4)	13.052(4)	12.887(3)
c, Å	9.109(3)	9.118(2)	9.084(3)
β, deg	100.401(15)	100.330(12)	100.549(12)
V, Å^3	1549.9(9)	1546.6(8)	1516.9(7)
Z	4	4	4
$D_{calcd.}$, g cm^{-3}	2.23	2.24	2.36
μ(MoK_α), cm^{-1}	4.0	4.3	5.8
F(000), e	1008	1012	1032
hkl range	±17, ±16, ±11	±17, ±16, −11 → +9	−16 → +17, ±16, ±11
θ_{max}, deg	3.12 – 27.48	3.12 – 27.47	3.14 – 27.49
Refl. measured/unique/R_{int}	14 169/3545/0.0314	14 259/3522/0.0317	14 019/3456/0.0472
Param. refined	244	241	244
$R(F)/wR(F^2)$ (all refls.)	0.0234/0.0596	0.0224/0.0547	0.0252/0.0601
GoF (F^2)	1.082	1.094	1.087
$\Delta\rho_{fin}$ (max/min), e Å^{-3}	1.39/−0.95	1.19/−0.84	1.64/−0.86

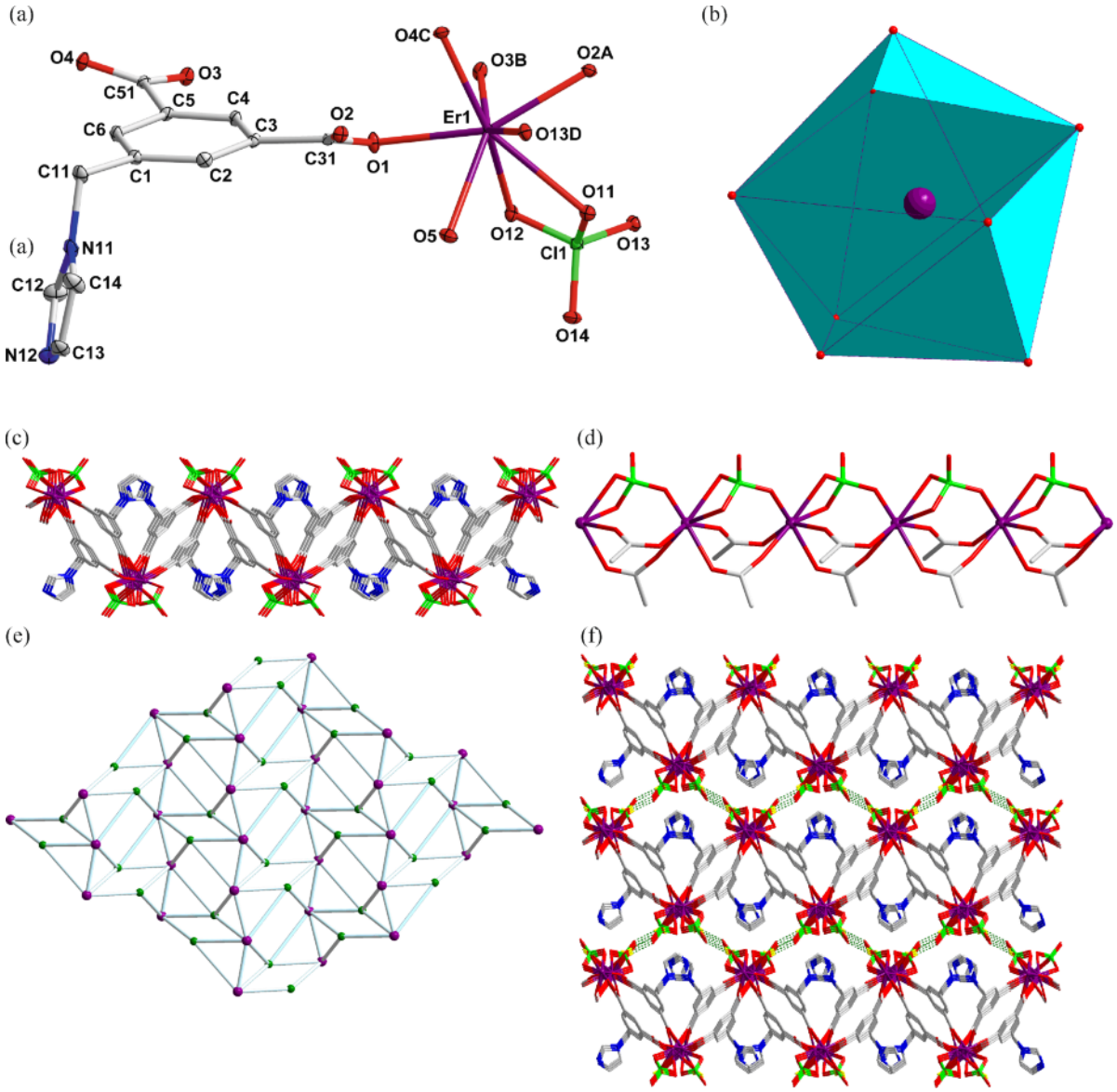

Fig. 1 (color online). (a) The coordination environment of Er(II) ions in **3** with ellipsoids drawn at the 30 % probability level. The hydrogen atoms and water molecules are omitted for clarity. (b) Polyhedral representation of [ErO_8]. (c) View of the 2D network of **3**. (d) The perchlorate- and carboxylate-bridged metal chain in **3**. (e) View of binodal (4,6)-connected 2D network of **3**. (f) View of the 3D supramolecular framework of **3** extended by hydrogen bonding interactions.

tion mode. Two perchlorate O atoms are attached to the Er(III) cation with a chelating angle of 57.16(7)°, while another O atom coordinates to a different Er(III) cation. So the perchlorate anion links two Er(III) ions as a μ_2-bridge. The interconnection between Er(III) and the *O*-donor groups of the perchlorate and L^{2-} anions forms a 2D wave-like network (Fig. 1c), within which there are perchlorate- and carboxylate-bridged metal chains (Fig. 1d).

Topology can be used to simplify the framework of **3**. Each Er(III) ion is coordinated by four L^{2-} ligands, and adjacent Er(III) ions are bridged by perchlorate anions, and thus, each Er(III) ion can be regarded as a 6-connector node. Each L^{2-} ligand as a μ_4-

Table 2. Selected bond lengths (Å) and angles (deg) for complexes **1**–**3**[a].

{[Sm(L)(OClO$_3$)(H$_2$O)]·0.5H$_2$O}$_n$ (**1**)			
Sm(1)–O(1)	2.298(2)	Sm(1)–O(5)	2.466(3)
Sm(1)–O(11)	2.452(2)	Sm(1)–O(12)	2.569(2)
Sm(1)–O(3)#1	2.435(2)	Sm(1)–O(4)#2	2.395(2)
Sm(1)–O(13)#3	2.454(2)	Sm(1)–O(2)#4	2.425(2)
O(1)–Sm(1)–O(5)	120.96(8)	O(4)#2–Sm(1)–O(13)#3	75.84(7)
O(11)–Sm(1)–O(12)	55.91(7)	O(1)–Sm(1)–O(3)#1	80.49(7)
O(1)–Sm(1)–O(4)#2	85.11(7)	O(1)–Sm(1)–O(13)#3	81.97(7)
O(1)–Sm(1)–O(2)#4	79.02(7)	O(5)–Sm(1)–O(13)#3	73.53(8)
O(2)#4–Sm(1)–O(3)#1	72.82(7)	O(3)#1–Sm(1)–O(5)	74.91(8)
O(2)#4–Sm(1)–O(4)#2	77.62(7)		
{[Eu(L)(OClO$_3$)(H$_2$O)]·0.5H$_2$O}$_n$ (**2**)			
Eu(1)–O(1)	2.285(2)	Eu(1)–O(5)	2.454(2)
Eu(1)–O(11)	2.438(2)	Eu(1)–O(12)	2.561(2)
Eu(1)–O(4)#1	2.422(2)	Eu(1)–O(3)#2	2.378(2)
Eu(1)–O(2)#3	2.413(2)	Eu(1)–O(14)#4	2.441(2)
O(1)–Eu(1)–O(5)	120.36(7)	O(3)#2–Eu(1)–O(14)#4	76.16(6)
O(5)–Eu(1)–O(14)#4	73.60(7)	O(1)–Eu(1)–O(4)#1	79.65(7)
O(1)–Eu(1)–O(3)#2	85.31(7)	O(1)–Eu(1)–O(2)#3	79.30(7)
O(1)–Eu(1)–O(14)#4	81.47(7)	O(11)–Eu(1)–O(12)	56.28(6)
O(2)#3–Eu(1)–O(4)#1	73.19(7)	O(4)#1–Eu(1)–O(5)	74.81(7)
O(2)#3–Eu(1)–O(3)#2	77.35(7)		
{[Er(L)(OClO$_3$)(H$_2$O)]·0.5H$_2$O}$_n$ (**3**)			
Er(1)–O(1)	2.362(2)	Er(1)–O(5)	2.393(3)
Er(1)–O(11)	2.539(2)	Er(1)–O(12)	2.374(2)
Er(1)–O(4)#1	2.234(3)	Er(1)–O(3)#2	2.342(2)
Er(1)–O(13)#3	2.374(2)	Er(1)–O(2)#4	2.302(2)
O(1)–Er(1)–O(5)	74.20(8)	O(2)#4–Er(1)–O(13)#3	76.50(7)
O(4)#1–Er(1)–O(13)#3	80.54(8)	O(1)–Er(1)–O(4)#1	78.52(8)
O(1)–Er(1)–O(3)#2	73.73(7)	O(5)–Er(1)–O(13)#3	73.40(8)
O(3)#2–Er(1)–O(4)#1	80.08(8)	O(11)–Er(1)–O(12)	57.16(7)
O(2)#4–Er(1)–O(4)#1	85.67(8)	O(4)#1–Er(1)–O(5)	118.84(9)
O(2)#4–Er(1)–O(3)#2	77.58(7)		

[a] Symmetry transformations used to generate equivalent atoms for **1**: #1 $1-x$, $1/2+y$, $1/2-z$; #2 $1-x$, $-y$, $1-z$; #3 x, $1/2-y$, $-1/2+z$; #4 x, $1/2-y$, $1/2+z$. For **2**: #1 $2-x$, $-1/2+y$, $3/2-z$; #2 $2-x$, $1-y$, $1-z$; #3 x, $1/2-y$, $-1/2+z$; #4 x, $1/2-y$, $1/2+z$. For **3**: #1 $2-x$, $1/2+y$, $1/2-z$; #2 $2-x$, $1-y$, $1-z$; #3 x, $3/2-y$, $-1/2+z$; #4 x, $3/2-y$, $1/2+z$.

bridge can be treated as a 4-connector node. Then, the structure of **3** can be simplified as a 2-nodal (4,6)-connected 2D network with $(3^2.4^2.5^2)(3^4.4^4.5^4.6^3)$ topology (Fig. 1e) [16]. When considering hydrogen bonding interactions [O(5)–H(10)···O(14)#1, #1: $1-x$, $1-y$, $1-z$; O(5)···O(14)#1 = 2.756(4) Å; ∠O(6)–H(17)–O(6)#1 = 175°], a 3D supramolecular framework is constructed (Fig. 1f).

PXRD and IR spectroscopy

The phase purity of **1**–**3** could be proven by powder X-ray diffraction (PXRD). As shown in Fig. 2, each PXRD pattern of the as-synthesized sample is consistent with the simulated one.

The deprotonation of H_2L to generate L^{2-} anions in **1**–**3** was confirmed by IR spectral data (see Experimental Section) since no characteristic vibration bands for carboxylic groups in the range of 1680 – 1760 cm^{-1} can be observed. For **1**–**3**, broad bands at 3400 cm^{-1} correspond to the vibrations of solvate water; bands at 1550 cm^{-1} are assigned to C–H stretches of benzene rings at L^{2-} anions.

Luminescence properties

Due to the outstanding luminescence properties of Eu(III), the photoluminescence of complex **2** was investigated in the solid state at room temperature. The emission spectrum is shown in Fig. 3. As an Eu(III) compound, complex **2** should exhibit five characteristic transitions of $^5D_0 \rightarrow {}^7F_J$ ($J = 0-4$), but in most cases, the $^5D_0 \rightarrow {}^7F_0$ transition is too weak to be observed [17, 18]. The emission spectrum of **2** upon ex-

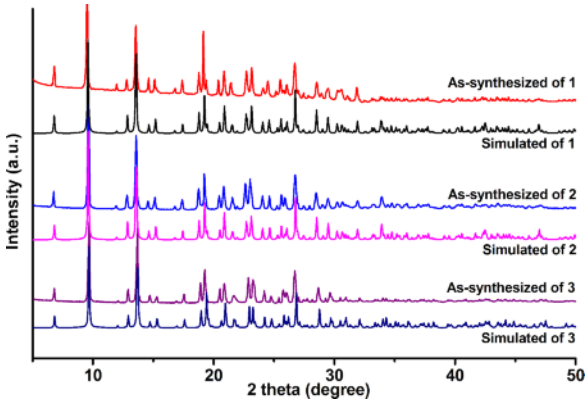

Fig. 2 (color online). The PXRD patterns of complexes **1**–**3**.

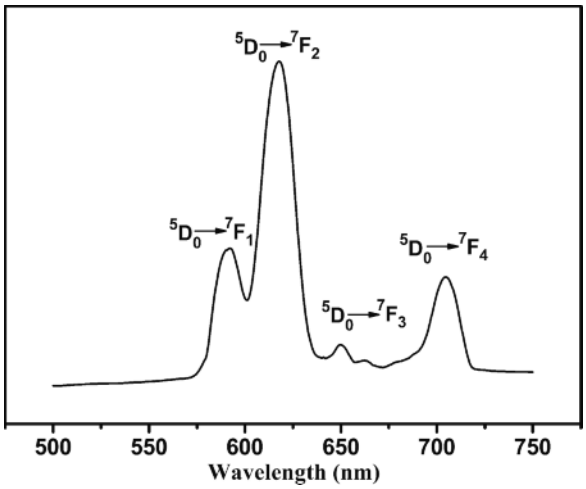

Fig. 3. The solid-state emission spectrum of **3** at room temperature.

citation at 391 nm shows four characteristic transitions of $^5D_0 \rightarrow ^7F_J$ ($J = 1-4$) at 591, 618, 650, and 704 nm. The most intense is the $^5D_0 \rightarrow ^7F_2$ transition, which can be attributed to the magnetic dipole transition [19, 20]. The result suggests that the ligand-to-metal energy transfer may be efficient under the experimental conditions [21, 22].

Conclusion

Three new lanthanide-organic frameworks $\{[Ln(L)(OClO_3)(H_2O)]\cdot 0.5H_2O\}_n$ [*Ln* = Sm (**1**), Eu (**2**), Er (**3**)] have been prepared by hydrothermal reactions of the corresponding lanthanide oxide (Ln_2O_3), silver perchlorate ($AgClO_4$) and 5-(imidazol-1-ylmethyl)isophthalic acid. Although not present in the complexes, silver ions have been proven to play a role in the formation of these 2D lanthanide-organic frameworks. Luminescence measurement revealed that complex **2** exhibits the characteristic emission bands of Eu(III) complexes, the strongest emission being due to the $^5D_0 \rightarrow ^7F_2$ transition at 618 nm.

Experimental Section

All commercially available chemicals were of reagent grade and used as received without further purification. The neutral H_2L ligand precursor was synthesized *via* the experimental procedure reported in the literature [13]. Elemental analyses of C, H, and N were taken on a Perkin-Elmer 240C elemental analyzer. Infrared spectra (IR) were recorded on a Bruker Vector22 FT-IR spectrophotometer using KBr pellets. Powder X-ray diffraction (PXRD) patterns were measured on a Shimadzu XRD-6000 X-ray diffractometer with CuK_α ($\lambda = 1.5418$ Å) radiation at room temperature. The luminescence spectrum for the powdered solid sample of **2** was measured on an Aminco Bowman Series 2 spectrofluorometer with a xenon arc lamp as the light source.

Preparation of $\{[Ln(L)(OClO_3)(H_2O)]\cdot 0.5H_2O\}_n$ *[Ln = Sm (**1**), Eu (**2**), Er (**3**)]*

The reaction mixture of 0.05 mmol Ln_2O_3 [17.4 mg (**1**), 17.6 mg (**2**), 19.1 mg (**3**)], $AgClO_4$ (20.7 mg, 0.1 mmol), and H_2L (24.6 mg, 0.1 mmol) in 10 mL H_2O was sealed in a 16 mL Teflon-lined stainless-steel container and heated at 140 °C for 72 h. Then the oven was cooled down at a rate of 10 °C h^{-1}. After cooling to room temperature, colorless platelets of **1**–**3** suitable for single-crystal X-ray diffraction were obtained.

For **1**: an approximate yield of 22 % based on H_2L. – $C_{24}H_{22}Cl_2N_4O_{19}Sm$ (1042.07): calcd. C 27.66, H 2.13, N 5.38 %; found C 27.92, H 1.88, N 5.16 %. – IR (KBr pellet, cm^{-1}): $\nu = 3404$ (m), 1609 (s), 1550 (s), 1445 (s), 1411 (s), 1381 (s), 1313 (w), 1280 (w), 1212 (m), 1094 (m), 1062 (s), 783 (w), 743 (w), 715 (w), 657 (w), 607 (w).

For **2**: an approximate yield of 30 % based on H_2L. – $C_{24}H_{22}Cl_2N_4O_{19}Eu$ (1045.28): calcd. C 27.58, H 2.12, N 5.36 %; found C 27.31, H 2.38, N 5.60 %. – IR (KBr pellet, cm^{-1}): $\nu = 3435$ (m), 1606 (s), 1548 (s), 1446 (s), 1412 (s), 1380 (s), 1311 (m), 1280 (m), 1209 (m), 1096 (m), 1061 (s), 743 (m), 713 (m), 656 (m), 610 (m).

For **3**: an approximate yield of 26 % based on H_2L. – $C_{24}H_{22}Cl_2N_4O_{19}Er$ (1075.87): calcd. C 27.79, H 2.06, N 5.21 %; found C 27.52, H 1.96, N 5.44 %. – IR (KBr pellet, cm^{-1}): $\nu = 3445$ (m), 1609 (s), 1558 (s), 1448 (s), 1414 (s), 1381 (s), 1279 (m), 1207 (m), 1098 (s), 1060 (s), 785 (m), 739 (s), 714 (m), 655 (m), 612 (m).

X-Ray structure determinations

The crystallographic data for complexes **1**–**3** were collected with a Rigaku Rapid II imaging plate area detector with MoK_α radiation ($\lambda = 0.71073$ Å) using a MicroMax-007HF microfocus rotating anode X-ray generator and VariMax-Mo optics at 200 K. The structures were solved by Direct Methods with SIR92 [23] and expanded using Fourier techniques [24]. All hydrogen atoms at C atoms were generated geometrically, while the hydrogen atoms at the water molecules could be found in reasonable positions in the difference Fourier maps (except those of the water of **2** which could not be located) and thus were excluded in the refinement (SHELXL-97 [25]). Some O–H distances were restrained *via* DFIX instructions. The details of crystal parameters, data collection, and refinements are summarized in Table 1, and selected bond lengths and angles are listed in Table 2.

CCDC 945201-945203 contain the supplementary crystallographic data for this paper. These data can be obtained free of charge from The Cambridge Crystallographic Data Centre *via* www.ccdc.cam.ac.uk/data_request/cif.

Acknowledgement

This work was financially supported by the special fund for the promotion program of industry university research cooperation of Huaian Administration of Science & Technology (HC201216).

[1] Z. M. Wang, K. L. Hu, S. Gao, H. Kobayashi, *Adv. Mater* **2010**, *22*, 1526 – 1533.
[2] T. Uemura, Y. Ono, Y. Hijikata, S. Kitagawa, *J. Am. Chem. Soc.* **2010**, *132*, 4917 – 4924.
[3] J. P. Zhang, Y. B. Zhang, J. B. Lin, X. M. Chen, *Chem. Rev.* **2012**, *112*, 1001 – 1033.
[4] A. Bétard, R. A. Fischer, *Chem. Rev.* **2012**, *112*, 1055 – 1083.
[5] B. L. Chen, S. C. Xiang, G. D. Qian, *Acc. Chem. Res.* **2010**, *43*, 1115 – 1124.
[6] J. R. Li, R. J. Kuppler, H. C. Zhou, *Chem. Soc. Rev.* **2009**, *38*, 1477 – 1504.
[7] M. S. Chen, J. Fan, T. A. Okamura, G. C. Lv, W. Y. Sun, *Inorg. Chim. Acta* **2011**, *366*, 268 – 274.
[8] X. J. Zheng, L. P. Jin, S. Gao, *Inorg. Chem.* **2004**, *43*, 1600 – 1602.
[9] X. Y. Chen, B. Zhao, W. Shi, J. Xia, P. Cheng, D. Z. Liao, S. P. Yan, Z. H. Jiang, *Chem. Mater.* **2005**, *17*, 2866 – 2874.
[10] L. F. Ma, L. Y. Wang, D. H. Lu, S. R. Batten, J. G. Wang, *Cryst. Growth Des.* **2009**, *9*, 1741 – 1749.
[11] Z. Su, J. Fan, T. A. Okamura, W. Y. Sun, N. Ueyama, *Cryst. Growth Des.* **2010**, *10*, 3515 – 3521.
[12] W. W. Zhou, J. T. Chen, G. Xu, M. S. Wang, J. P. Zou, X. F. Long, G. J. Wang, G. C. Guo, J. S. Huang, *Chem. Commun.* **2008**, 2762 – 2764.
[13] H. W. Kuai, J. Fan, Q. Liu, W. Y. Sun, *CrystEngComm* **2012**, *14*, 3708 – 3716.
[14] H. W. Kuai, C. Hou, W. Y. Sun, *Polyhedron* **2013**, *52*, 1268 – 1275.
[15] H. W. Kuai, X. C. Cheng, X. H. Zhu, *Inorg. Chem. Commun.* **2012**, *25*, 43 – 47.
[16] V. A. Blatov, *IUCr CompComm Newsletter* **2006**, *7*, 4 – 38.
[17] M. S. Chen, Z. Su, M. Chen, S. S. Chen, Y. Z. Li, W. Y. Sun, *CrystEngComm* **2010**, *12*, 3267 – 3276.
[18] P. P. Bartelemy, G. R. Choppin, *Inorg. Chem.* **1989**, *28*, 3354 – 3357.
[19] G. R. Choppin, D. R. Peterman, *Coord. Chem. Rev.* **1998**, *174*, 283 – 299.
[20] A. De Betterncount Dias, S. Viswanathan, *Chem. Commun.* **2004**, 1024 – 1025.
[21] X. J. Zheng, C. Y. Sun, S. Z. Lu, F. H. Liao, S. Gao, L. P. Jin, *Eur. J. Inorg. Chem.* **2004**, 3262 – 3268.
[22] M. Chen, M. S. Chen, T. A. Okamura, M. F. Lv, W. Y. Sun, N. Ueyama, *CrystEngComm* **2011**, *13*, 3801 – 3810.
[23] A. Altomare, G. Cascarano, C. Giacovazzo, A. Guagliardi, M. Burla, G. Polidori, M. Camalli, *J. Appl. Crystallogr.* **1994**, *27*, 435.
[24] P. T. Beurskens, G. Beurskens, R. de Gelder, S. García-Granda, R. O. Gould, R. Israel, J. M. M. Smits, The DIRDIF-99 Program System, Technical Report of the Crystallography Laboratory, University of Nijmegen, Nijmegen (The Netherlands) **1999**.
[25] G. M. Sheldrick, *Acta Crystallogr.* **2008**, *A64*, 112 – 122.